Mausam, (1988), 39, 3, 295-300

551.510.522 : 551.513.1

Step boundary conditions in the barotropic model

E. BUENDIA, F. VILLICANA, A. GALLEGOS*, O. DELGADO and E. DEL VALLE

Centro de Ciencias de la Atmosfera, UNAM

(*Received 28 August 1985*)

सार — सीमा प्रभावों पर रोक लगाने के लक्ष्य और क्षेत्र IV के लिये मौसम पूर्वानुमान कुशलता को बढ़ाने के ध्येय से पद सीमा स्थितियों को प्रस्तुत किया गया है और (दाब घनत्वी निदर्श भूविक्षेपी भ्रमिलता समीकरण पर आधारित) संख्यात्मक मॉडल पर परिवर्तित चक्रीयता स्थिति को संयुक्त रूप से लागू किया गया है। इससे प्रोत्साहिक परिणाम प्राप्त हुए जो कि इस बात की ओर संकेत करते हैं कि यद्यपि चक्रीयता स्थिति लागू हो सकती है परन्तु अपेक्षाकृत अच्छे अल्पकालिक मौसम पूर्वानुमान के लिये इसमें संशोधन किया जाना चाहिये।

ABSTRACT. Step boundary conditions (SBC) are introduced and, jointly with a modified cyclicity condition, have been implemented to a numerical model (based on the barotropic quasi-geostropic vorticity equation) in order to restrict boundary effects and improve the weather forecasting skill for Region IV. Encouraging results were obtained which indicate that the cyclicity condition, although applicable, should be revised to produce even better short-range weather predictions.

1. Introduction

The physical basis of the numerical weather prediction at synoptic scale was introduced by Charney in 1949. In the following year, Charney *et al.* (1950) published the first numerical weather forecast using the barotropic vorticity equation. They simplified the hydrodynamic equations, assuming a geostrophic balance while using the hydrostatic approximation and the divergence relation. With these simplifications they surmounted the integration difficulties that Richardson (1922) had by filtering out the numerical noise produced by the propagation of high frequency acoustic and gravity waves. Shuman (1957) developed numerical methods to solve the balance equations and produced weather forecasts, which smoothly evolved from initial meteorological fields for a zonal belt. Shuman and Vanderman (1966) solved the primitive equation for the zonal belt between 45°S and 45°N. Other numerical integrations for the northern hemisphere (Phillips 1959) and for the terrestial globe (Kasahara 1977) were also conducted with encouraging results.

Asnani (1972), Mukerji and Datta (1973), Sikka (1975) and Ramanathan and Bansal (1977) have developed numerical models to produce short range weather forecasts for India and its surrounding areas. The numerical experiments demonstrate that these models suitably predict the evolution of low pressure systems, the occurrence of monsoons and the trajectories of tropical cyclones. Bedi (1979), applying a spectral technique to integrate the primitive equations of a barotropic numerical model, extended weather predictions to the northern hemisphere.

Similar numerical weather predictions experiments have been conducted in Mexico for a limited geographical area — Region IV — as described by Buendia *et al.* (1976-77), Buendia *et al.* (1979) and Buendia and Delgado (1981). The main problems that arose in all of these experiments were the boundary conditions effects. As pointed out by Charney *et al.* (1950), boundary effects drastically reduce the accuracy of numerical weather forecasts.

A procedure is introduced in the present work to decrease the negative effects created at the boundaries of the geographical area considered for the numerical weather predictions. The basic idea is to take advantage of the average meteorological conditions of Region IV, limited to the west by the Pacific high and to the east by the Atlantic high, persistent westerlies to the north and equally persistent easterlies to the south. This circumstance tolerates the prescription of a cyclicity condition along the eastern (meridional) boundary of Region IV and uniform zonal flows along the north and south (latitudinal) boundaries of the same region.

2. The model

The fundamental equation of the model is the quasi-geostrophic vorticity equations (Buendia *et al.* 1976-77):

$$m^2 \frac{\partial \nabla^2 Z}{\partial t} = - \left| \frac{g}{f} m^2 J(Z, m^2 \nabla^2 Z) + m^2 \frac{\partial f}{\partial y} \frac{\partial Z}{\partial x} \right| \tag{1}$$

where, m is the scale parameter of the Mercator projection (fixed at the equator) for an area including

*Instituto de Ciencias del Mar y Limnologia, UNAM

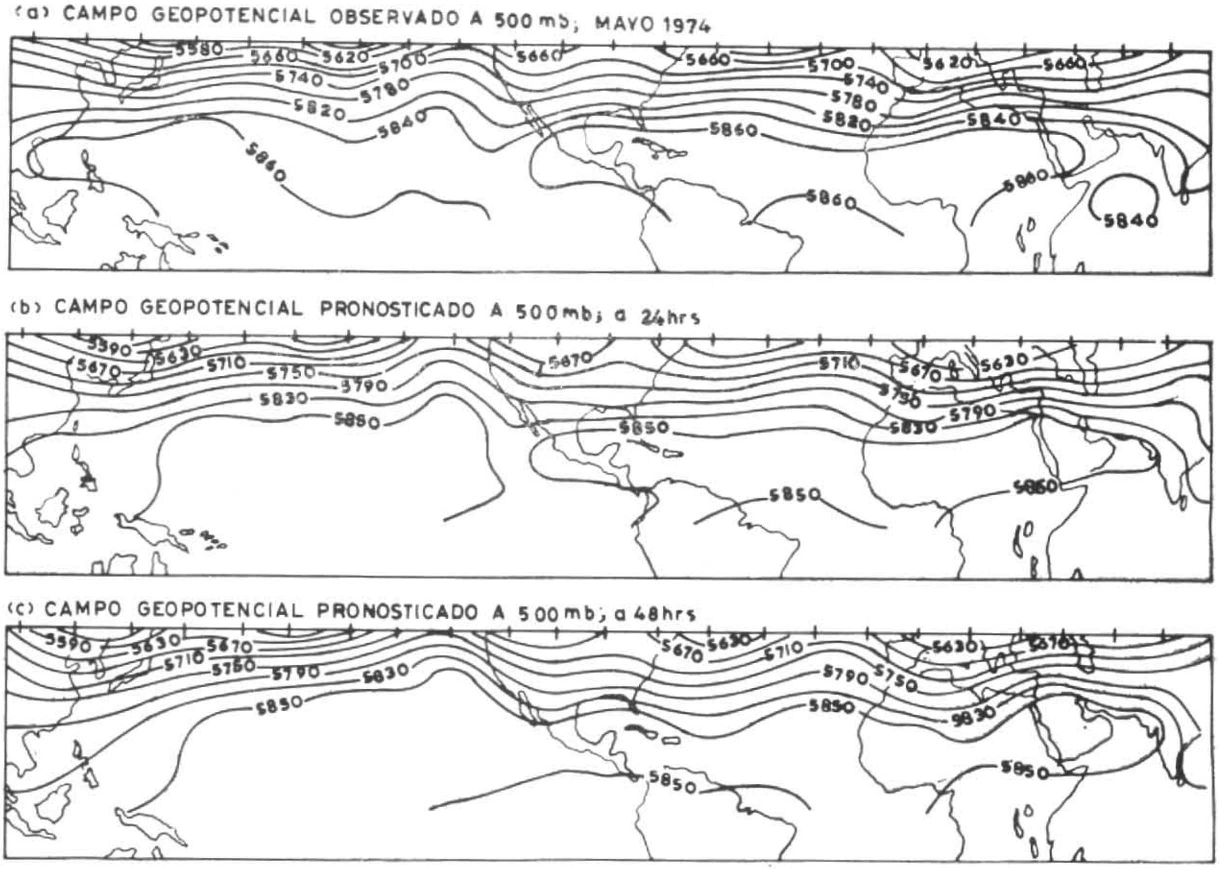

Figs. 1(a-c). Isohiptic field at 500 mb for the month of May 1974 : (a) average, (b) 24-hr forecast and (c) 48-hr forecast

Region IV, Z is the 500 mb geopotential height, g is the gravity acceleration, f is the Coriolis parameter, ∇^2 is the horizontal Laplacian operator and J (,) is the Jacobian operator. The space-time variables are x, y and t; x positive to the east and y positive to the north.

(a) *Latitudinal boundary conditions*

Mass flux across east-west boundaries of the zonal belt considered (5°S and 50°N) is constrained to zero. Therefore, the boundary condition imposed along these latitudes, is of geopotential constant value.

A non-uniform flow parallel to a fixed boundary creates an expanding boundary layer, where turbulent motions of increasing space-time scales are generated. These non-linear interactions diffuse into the forecast region (Elliasen 1956). To avoid the analog of this effect in the numerical model, the zonal flow near the latitudinal boundaries (at 5° S and 50° N) should be null. Accordingly, a zero gradient of the 500 mb geopotential height is prescribed for the first three grid points in the y direction for each column of the grid from both the north and south boundaries towards the interior of the zonal belt.

The imposed boundary conditions described above are applied in alternate succesion. Thus, they will be referred to as step boundary conditions (SBC).

(b) *Meridional conditions*

The east Pacific high and the Altantic high form the boundaries of Region IV to the east and to the west, respectively. These high semi-permanent pressure systems are associated with persistent westerly winds at high latitudes of Region IV and equally persistent easterly winds at lower latitudes of this same region. This situation admits a cyclicity condition between the eastern and western limits of Region IV.

Faulkner (1976) applied this natural condition for a global (complete) zonal belt.

In the present case the cyclicity condition is used as if the eastern and western ends of Region IV closed to form a cylindrical surface.

(c) *Integration of the model equation*

Following Arakawa (1976), the Jacobian in Eqn. (1) is numerically manipulated in such a way that it conserves vorticity and kinetic energy. The relaxation method used to solve Eqn. (1) is described in Carnahan *et al.* (1969) and predicts the tendency of the 500 mb geopotential height.

The forecasts were obtained in the traditional way using the relation :

$$Z(t+1) = Z(t) + \triangle t \left(\frac{\partial Z}{\partial t}\right) \quad (2)$$

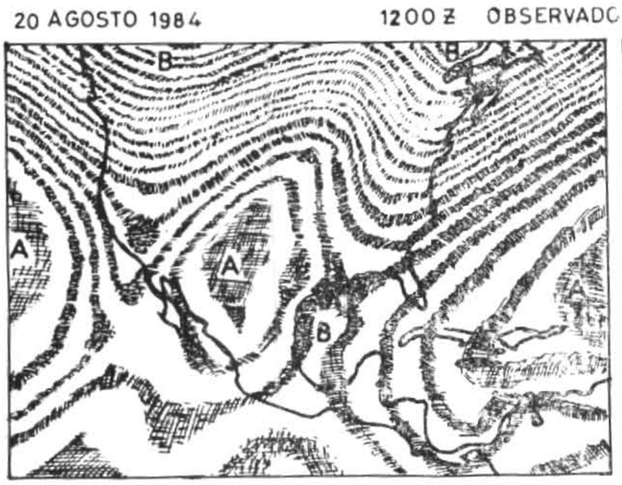

Fig. 2(a). Observed field of the 500 mb geopotential height at 1200 GMT on 20 August 1984

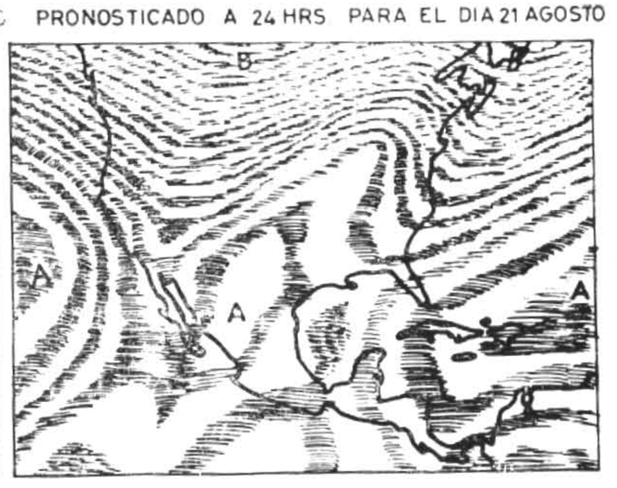

Fig. 2(b). 24-hr forecast of the field

for the initial time step and central differences for subsequent time steps. The time step interval was 1 hour.

The distance between consecutive gridpoints in Region IV is 463 km in both the x and y directions. This grid is similar to that used by Mukerji and Datta (1973). In the present work, five columns of gridpoints were added to the east of Region IV in order to smooth out the cyclicity condition. The zonal belt that contains Region IV has a grid that consists of 5° latitude-5° longitude squares.

3. Results and discussion

The stability of the numerical model under the SBC was tested *via* an experiment, where the initial conditions were isohiptic field data averaged over a month. The experiment was conducted for a global zonal belt (*i.e.*, under natural cyclicity conditions) and concluded after one hundered 1-hour time steps. The boundary effects were apparently constrained to the north and south latitudinal boundaries in view of the fact that throughout the stability test the model performed close to what normally is observed departing from similar initial conditions. The following paragraphs and Figs. 1 (a-c) describe this experiment and its results.

Fig. 1 (a) shows the average isohiptic field at 500 mb for the month of May 1974. In it, weak troughs along the eastern coasts of North America and Asia are observed. More definite troughs are evident over western Africa, western North America and eastern India. A high geopotential value is notoriously present along the tropical belt.

In the 24-hr and 48-hr forecasts of the initial isohiptic field (Figs. 1 a-c respectively) and eastward displacement of 5° longitude per day of the weak eastern trough over North America is noted. At the same time, the weak trough initially over east Asia moved west towards central Asia. By comparing Figs. 1 (a-c) a low pressure system over the Indian Ocean is weakened by the monsoonic flux.

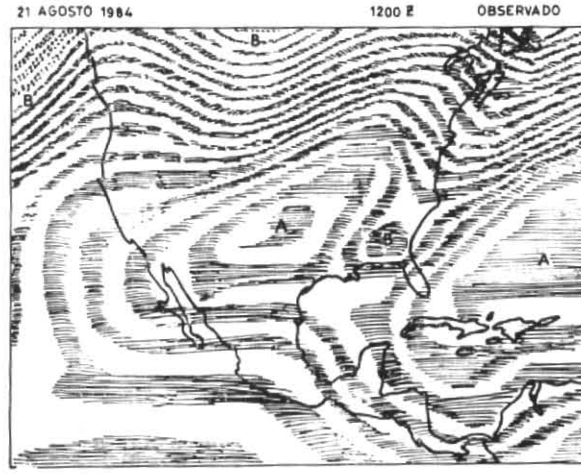

Fig. 3. Observed isohiptic field of the 500 mb geopotential height, at 1200 GMT on 21 August 1984

The 500 mb observed at 1200 GMT on 20 August 1984, and 24-hr forecasted field are shown in Figs. 2 (a & b) respectively. Two deep troughs were observed to the east and to the west of Canada and the U.S.A. and an anticyclonic system was observed over northern Mexico. This situation produced a ridge separating the observed troughs.

The 24-hr forecast of the isohiptic field (Fig. 2b) exhibits an eastward displacement of the troughs and the continental ridge. This is consistent with the observed field on 21 August 1984 at 1200 GMT as shown in Fig. 3.

By using the data of the 21 August 1984 (Fig. 3) as the initial isohiptic field, the solution of Eqn. (1) forecasts (Fig. 4) : (*i*) a cyclonic system north of Florida (U.S.A.) (*ii*) a trough over east-central Canada and U.S.A., (*iii*) a ridge over the west-central

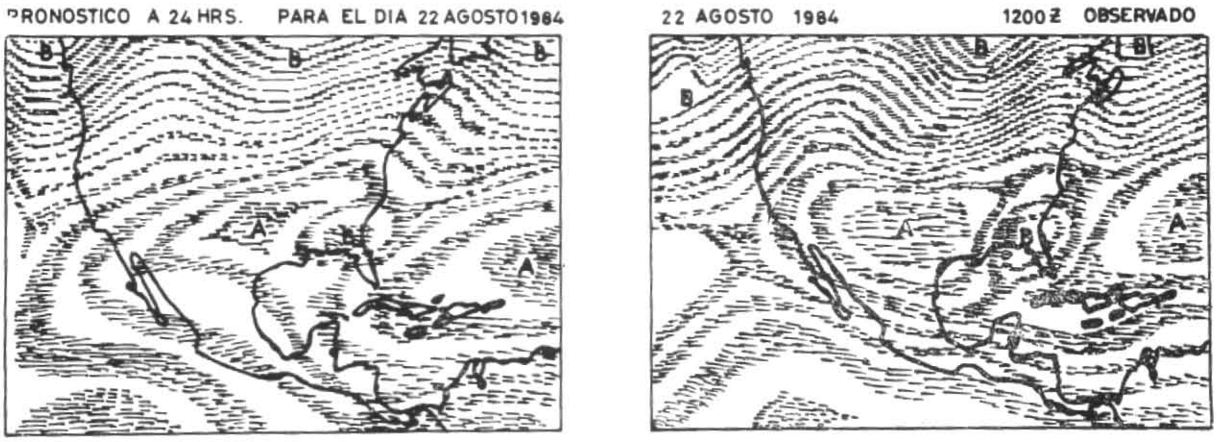

Fig. 4. 24-hr forecast of the field of the 500 geopotential height at 1200 GMT on 22 August 1984

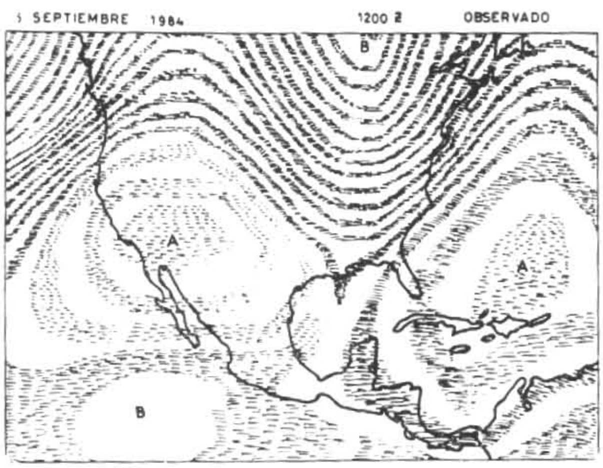

Fig. 5. Observed isohiptic field of 500 mb geopotential height at 1200 GMT on 5 September 1984

part of this same region and (*iv*) a high pressure system slightly displaced to the south in relation to its observed position the day before as (Fig. 3) within the anticyclonic circulation of the observed field of the next day (22 August 1984).

The 500 mb isohiptic field observed on the 5 September 1984, at 1200 GMT is displayed in Fig. 5. A deep trough north of the Gulf of Mexico (reaching Canadian latitudes) and an anticyclone north of the Gulf of California are the two predominant atmospheric systems. This figure also exhibits : (*i*) an anticyclonic system north of Haiti, (*ii*) a cyclonic system in the north eastern tropical Pacific and (*iii*) a dominant southeasterly flow on the western side of Region IV, north of 35°N.

The 24-hr forecasts for 5 September 1984, are shown in Fig. 6 (a). It shows a coherent eastward displacement of the atmospheric system along the middle and northern latitudes of Region IV. The trough observed on the 5 September 1984, north of the Gulf of Mexico (Fig. 5) appears, on this forecast (Fig. 6 a), over the east coasts of the U.S.A. and Canada. The accuracy of the 24-hr forecast is confirmed in the observed field on the 6 September 1984 (Fig. 6 b). Furthermore, comparing Figs. 6(a) and 6(b), the following similarities become clear : (*i*) The southeasterly flow initially on the western side of Region IV (Fig. 5) now forms part of the western trough, (*ii*) the cyclonic system initially over the north-eastern tropical Pacific (Fig. 5) has moved to the north and (*iii*) the anticyclonic system initially observed north of Haiti (Fig. 5) has moved to the north and (*iv*) the anticyclonic system, initially observed north of Haiti (Fig. 5) moved north and displaced the easterly winds away from the Gulf of Mexico.

The forecasts for the geopotential field (relative to 500 mb) under boundary conditions, similar to those used by Mukerji and Datta (1973) (hereafter denoted by MD 73) are approximately the same as those that result when SBC are used.

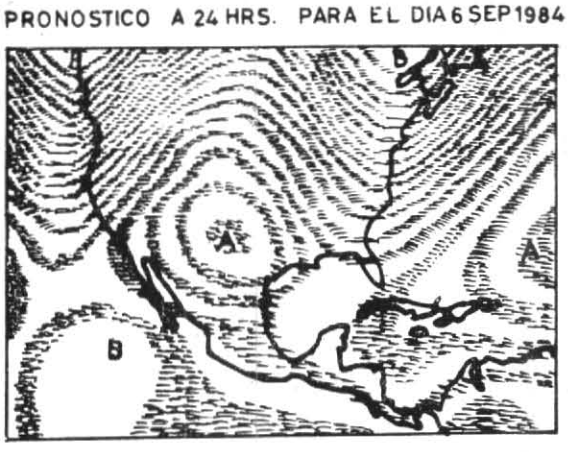

Fig. 6(a). 24-hr forecast of the field described in Fig. 5

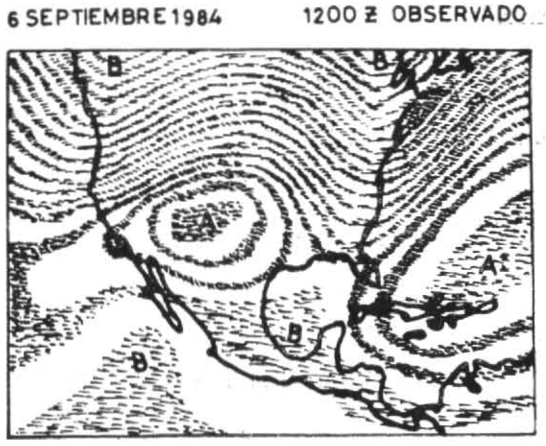

Fig. 6(b). Observed field of the 500 mb geopotential height at 1200 GMT for 6 September 1984

TABLE 1

Statistics of the forecasts for the days reported in the text

Day	RMSE (metres)			CI			SCS (%)	
	SBC	MD73	*P*	SBC	MD73	*P*	SBC	MD73
21 August 1984	27.40	26.37	40.77	0.888	0.885	0.740	64.65	64.65
22 August 1984	30.47	31.81	29.70	0.842	0.833	0.809	53.54	52.53
6 September 1984	36.38	38.22	58.78	0.934	0.927	0.781	64.65	64.65

RMSE=Root mean square error CI=Correlation Index

SCS=Success in the change of sign (Adem 1981) SBC=Step boundary conditions

MD73=Boundary conditions used by Mukerji and Datta and others *P*=Persistence

The difference between using SBC or other boundary condition resides in the improvement of a few geopotential metres, as shown in the statistics of the forecasts : (*i*) Root Mean Square Error (RMSE), (ii) Correlation Index (CI) and (*iii*) Success in the change of sign (SCS) [Adem 1981].

This occurred in 95% of the forecasts realized in the Centro de la Atmosfera (UNAM, Mexico) when using SBC.

Table 1 shows the statistics corresponding to the forecasts for the days reported in the present work using SBC and the boundary conditions using MD 73.

Starting the second half of 1984, the 24-hr forecasts implemented with the SBC are routinely produced as the Centro de Ciencias de la Atmosfera (UNAM, Mexico). These 24-hr forecasts reveal an acceptable degree of accuracy. Usually, the results show only the normal differences with the corresponding observed fields.

In light of the results described above, a similarity analysis will be carried out to improve the skill of the numerical model, considering that the cyclicity condition affects the absolute vorticity of the atmospheric systems propagating through Region IV (the cyclicity condition is equivalent to a reduction in length of the corresponding zonal belt). Also, future work will proceed to extend the 24-hr forecasts to the west of Region IV.

Acknowledgements

The authors wish to thank Mr. Rodolfo Meza and Miss Ma. Luisa Gonzalez for their collaboration, and wish to recognize the efficient services provided by the

computer center of the Universidad Nacional Autonoma de Mexico.

References

Adem, J. and Donn, W.L., 1981, *Progress in Monthly Climate Forecasting with a Physical Model*, Amer. Met. Soc., **62**, 12, pp. 1666-1675.

Arakawa, A., 1966, Computational design for long-term integration of the equation of fluid motion : Two-dimensional incompressible flow, Part I, *J. Comp. Phys.*, **1**, pp. 119-143.

Asnani, G.C., 1972, An experiment with barotropic quasi-geostropic model for the Indian region, *Indian J. Met. Geophys.*, **23**, 2, pp. 173-175.

Bedi, H.S., 1979, Spectral integration of a hemispheric model, *Mausam*, **30**, 1, pp. 31-38.

Buendia, E., Morales, T. *et al.*, 1976-77, Integracion numerica preliminar del modelo barotropico en la region IV. Parte I, *Anales del Instituto de Geofisica*, **22-23**, pp. 131-144.

Buendia, E., Morales, T. and Revilla, R., 1979, El Modelo barotropico equivalente en la Region IV, *Revista de Geofisica IPGH*, **10-11**, pp. 23-28.

Buendia, E. and Delgado, O., 1981, Integracion del modelo baroclinico filtrado en la cuarta region, *Revista de Geofisisa-IPGH*, **14-15**, pp. 153-169.

Carnahan, B., Lauther, H. and Wilkes, 1979, *J. Applied Numerical Methods*, John Wiley and Sons Inc., 604 pp.

Charney, J. G., 1949, On a physical basis for numerical prediction of large-scale in the atmosphere, *J. Met.*, **6**, pp. 371-385.

Charney, J. G., Fjortoft, R. and Von Newmann, J., 1950, Numerical integration of the barotropic vorticity equation, *Tellus*, **2**, pp. 237-254.

Eliassen, A., 1956, A procedure for numerical integration of the primitive equations of the two-parameter model of the atmosphere, *Sci. Rep.* No. 4, Dept. of Meteorology, UCLA 1.

Faulkner, F.D., 1976, The numerical solution of the Helmholtz equation on a sphere. NPS-53F a 76025, Naval Post-graduate School, Monterey, Calif. 1.

Kasahara, A., 1977, Numerical integration of the global barotropic primitive equation through harmonic expansions, *J. atmos. Sci.*, **34**, 5, pp. 687-701.

Mukerji, T. K. and Datta, R. K., 1973, Prognosis by four-layer quasi-geostrophic model, *Indian J. Met. Geophys.*, **24**, 2, pp. 93-100.

Phillips, N. A., 1959, Numerical integration of the primitive equation on a hemisphere, *Mon. Weath. Rev.*, **87**, 9, pp. 333-345.

Ramanathan, Y. and Bansal, R.K., 1977, On application of a primitive equation barotropic model for the prediction of storm tracks in the Indian region, *Indian J. Met. Hydrol. Geophys.*, **28**, 2, pp. 169-176.

Richardson, L., 1922, *Weather prediction by numerical process*, Cambridge Univ. Press, London and New York, 236 pp.

Shuman, F., 1957, Numerical methods in weather prediction, I : The balance equation, *Mon. Weath. Rev.*, **85**, 9, pp. 329-332.

Shuman, F., 1957, Numerical methods in weather prediction, II : Smoothing and filtering, *Mon. Weath. Rev.*, **85**, 11, pp. 357-361.

Shuman, F. and Vanderman, L., 1966, Difference system and boundary conditions for the primitive equation barotropic forecasts, *Mon. Weath. Rev.*, **94**, 5, pp. 329-335.

Sikka, D. R., 1975, Forecasting the movement of tropical cyclones in the Indian seas by non-divergent barotropic model, *Indian J. Met. Hydrol. Geophys.*, **26**, 3, pp. 323-325.